




Coronavirus Diagnosis Based on Chest X-Ray Images and Pre-Trained DenseNet-121

Yousra Kateb^{*}, Hocine Megloulou^{}, Abdelmalek Khebli^{}

Laboratory of Electrification of Industrial Enterprises, Faculty of Hydrocarbons and Chemistry, University of M'hamed Bougarra Boumerdes, City of the Independence, Boumerdes 35000, Algeria

Corresponding Author Email: y.kateb@univ-boumerdes.dz



<https://doi.org/10.18280/ria.370104>

ABSTRACT

Received: 29 November 2022

Accepted: 5 January 2023

Keywords:

chest X-ray, Convolutional Neural Network, COVID-19 diagnosis, DenseNet-121, image classification, small dataset

A serious global problem called COVID-19 has killed a great number of people and rendered many projects useless. The obtained individual's identification at the appropriate time is one of the crucial methods to reduce losses. By detecting and recognizing contaminated individuals in the early stages, artificial intelligence can help many associations in these situations. In this study, we offer a fully automated method to identify COVID-19 from a patient's chest X-ray images without the need for a clinical expert's assistance. The proposed approach was evaluated on the public COVID-19 X-ray dataset that achieves high performance and reduces computational complexity. This dataset contains 400 photos, 100 images of individuals who were infected with Covid-19, 100 images of individuals with no COVID-19, 100 images of a viral pneumonia and a 100 more images that we reserve them for testing part. So we have an overall 300 images for training and 100 for testing. The obtained results were so satisfying, an F1 score of 0.98, a Recall of 0.98, and an Accuracy of 0.98. The classification method deep learning-based DenseNet-121, transfer learning, as well as data augmentation techniques were implemented to improve the model more accurately. Our proposed approach outperforms several CNNs and all recent works on COVID-19 images. Even though there are not enough training photos comparing to other extra-large datasets.

1. INTRODUCTION

As of June 8 in 2021, Coronavirus disease 2019 (COVID-19), an infectious disease, had infected more than 174 million people worldwide and claimed more than 3.74 million lives [1]. The inefficiency and lack of diagnostics is one of the biggest obstacles to stop the development of this disease. Reverse transcription polymerase chain reaction is the primary technology used in current tests (RT-PCR). In comparison to the COVID-19 rapid spreading rate, it takes four to six hours to receive the results. In addition to being ineffective, RT-PCR test units are extremely scarce. As a result, many infected instances cannot be easily identified and continue to unintentionally infect others.

While (RT-PCR) has been regarded as the best quality level for SARS-CoV-2 analysis, the extremely limited stock and strict requirements for research facility climate would extraordinarily defer the precise finding of suspected patients, which has presented remarkable difficulties to stop the spread of the infection, especially at the focal point of the pandemic region. It's interesting that by combining the patient's clinical signs and symptoms with their new close contact, travel background, and research center findings, X-ray chest image diagnosis is a quick and efficient and simpler technique for clinical conclusion of COVID-19. This makes it possible for a quick determination as ahead of schedule as possible in the clinical practice. It is also helpful in controlling the plague, especially inside the confines of Wuhan, Hubei area, by timely removing affected patients. In other words, a chest X-ray is a crucial part of the symptomatic technique for suspected

patients, and several recent papers have highlighted its symptoms [2-6].

Deep learning, the primary advancement of the recently developing artificial intelligence (AI), has been accounted for in clinical imaging for the pre-programmed detection of lung diseases [7-9]. It demonstrated dermatologist-level performance on ordering skin lesions in 2017 [10], outperformed human-level execution on the ImageNet image classification task with 1,000,000 pictures for training in 2015 [11], and obtained remarkably good results for cellular breakdown in the lungs separating 2019 [7]. As a result, our goal is to apply a deep learning model to determine whether COVID-19 is present in the X-ray pictures or not. The Densely Connected Convolutional Networks DenseNet121 model will be used in this study because of its benefits, including high accuracy, capacity, parameter efficiency, and the ability to address the overfitting issue.

This paper is structured as follows: The most recent and well-liked relevant works are reviewed in Section 2, our approach is put into practice in Section 3, and the results and discussion are covered in Section 4. Our paper is finished with a conclusion section.

2. RELATED WORK

Since the COVID-19 outbreak, scientists have done many efforts to develop new deep learning techniques that perform COVID-19 screening depending on medical images, such as CT scans and chest X-rays have increased. To describe CT

sweeps of patients with COVID-19, Wu et al. [12] set up an early screening model that is dependent on various CNN models. Chest CT cuts were used by Wang et al. [13] to propose a 3D deep CNN (DeCoVNet) to detect COVID-19. Based on chest X-ray images, Chowdhury et al. [14] used CNN to identify COVID-19 patients. In other publications, 3D deep learning models have also been used to screen COVID-19 based on chest CT data [15, 16]. To assist doctors in differentiating patients with COVID-19, Yang et al. [17] developed the Deep Pneumonia CT detection framework (based on deep learning). By modifying the origin transfer learning model to provide a clinical conclusion prior to the pathogenic test, Xu et al. [18] established a deep learning algorithm. Shi et al. [19] used the "VB-Net" neural network to delineate the locations of COVID19 infection in CT scans. Yu et al. [20] created a framework based on UNet++ for the purpose of identifying COVID-19 from CT images. An infection-size-aware Random Forest (iSARF) method was presented by Shen et al. [21] and can automatically group participants into bunches depending on the size of an infected sore. For finding the presence of COVID-19 in chest X-ray pictures, Wang et al. [22] presented an MAI-Nets model. A CFW-Net deep learning model was proposed by Wang et al [23]. To identify the COVID-19, Wang et al. [24] developed the Wavelet Renyi Entropy and Three-Segment Biogeography-Based Optimization model.

3. EXPERIMENTATION PART

3.1 Materials and methods

3.1.1 Dataset preparation and pre-processing

In this work, two open source datasets were used [25, 26]. In order to remove the noise caused by patients moving during analysis, we downscaled the image in this test to 128x128 and then applied the Gaussian channel. The knowledge has also been rearranged throughout the instruction at each age. The informational index is divided into two parts: training accounts for 80% and approval for 20%. From that point on, we expand the information using a variety of strategies, including flipping vertically and horizontally, rotating at various angles, shifting the width and height by around 0.2, and trimming 0.1 of the images, in order to reduce over-fitting while also increasing the informational collection. Figure 1 shows the examples of normal (top) and Coronavirus (bottom) images present in the dataset, respectively. It can be noted that on the thoracic X-rays of patients with COVID-19 pneumonia, there is an increase density (whiter) of the lungs. Usually, the more severe the disease, the more intense the whiteness on chest X-rays as shown in Figure 2.

3.1.2 Transfer learning

When doing transfer learning, a convolutional neural architecture is used combined with pre-trained loads from large-scale datasets, such as ImageNet [27], and the loads are then adjusted for the target task. Both linguistic cognizance [28] and visual acknowledgment [29] have successfully used this idea. Transfer learning has also been widely applied to medical picture classification and acknowledgment assignments, such as tumor classification [30], the conclusion of retinal infections [31], pneumonia detection [32], and classification of skin lesion and malignant growth [33, 34]. We make use of an open source dataset [35, 36] that consists of

COVID, Pneumonia, and standard X-ray pictures. There are 400 photos in total. Our data is divided into three groups: 100 samples for the typical X-ray images, 100 samples for pneumonic images, and 100 samples for Covid-19 images.

Figure 2 shows various sample photos that were labeled by knowledgeable professors as normal (left) or COVID-19 cases (right).

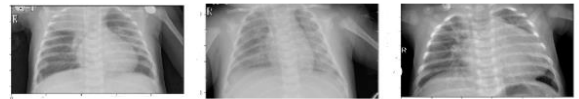


Figure 1.a.



Figure 1.b.

Figure 1. Different positions of sample images with Covid (Figure 1.a) and without COVID-19 (Figure 1.b) after pre-processing

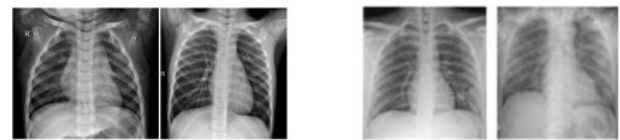


Figure 2. Chest X-Ray sample images: 'Normal' (left) and 'COVID-19' (right)

3.1.3 DenseNet-121 architecture

A potent technology with numerous practical uses is deep neural networks (DNN) [37]. This section describes the transfer learning-based CNN model that has been certified for the classification of images as normal or COVID-19. We first re-sampled all photos to 128x128 in accordance with the architecture being used. As previously mentioned, we employed established networks like DenseNet-121 to achieve our goals of transfer learning. We may keep a wealth of knowledge for classifying different artefacts from prior training by using these well-trained networks. Layers and weights are kept intact until the last fully linked layer.

We will update DenseNet-121 with our data. 1000 classes have been trained using DenseNet's 121 million photo database. In our instance, we have three classes and 400 photos. We replaced the last three layers with a Softmax layer to make the classification of our own dataset (Figure 3).

Each layer is linked to every other layer in a DenseNet architecture, giving rise to the term densely connected convolutional network. There are $L(L+1)/2$ direct connections for L layers. The feature maps of all the layers before it are used as inputs for each layer, and its own feature maps are utilized as inputs for each layer after it. In essence, DenseNets link each layer to every other layer. The main, incredibly potent idea is this. An input layer in DenseNet is created by concatenating feature maps from earlier layers (Table 1). "DenseNets offer numerous compelling advantages: they ease the vanishing-gradient problem, strengthen feature propagation, stimulate feature reuse, and drastically reduce the number of parameters," according to the paper on densely connected convolutional networks [38].

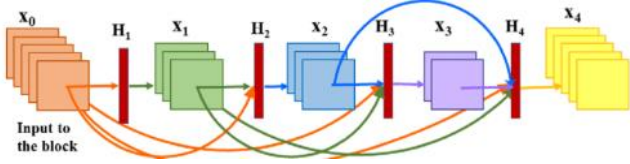


Figure 3. DenseNet architecture

Table 1. DenseNet-121 parameters summary

Layer (type)	Output Shape	Parameters
Efficientnet-b7	(none, 16, 16, 2560)	64097680
Global average pooling2d	(G1 (None, 2560))	0
Dense	(None, 104)	266344
Total parameters	64,364,024	
Trainable parameters	266,344	
Non-trainable parameters	64,097,680	

Traditional convolutional feed-forward networks connect the output of the $(L)^{th}$ layer as input to the $(L + 1)^{th}$ layer [39] which gives rise to the following layer transition: Eq. (1).

$$x_L = H(x_{L-1}) \quad (1)$$

In DenseNet architecture, the dense connectivity equation is defined in Eq. (2).

$$x_L = H([x_0, x_1, x_2, \dots, x_{L-1}]) \quad (2)$$

where, $[x_0, x_1, x_2, \dots, x_{L-1}]$ represents concatenation of the feature maps produced by $[0, 1, L^{th}]$ layers (Figure 4).

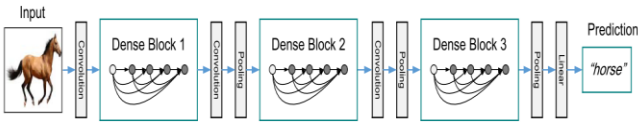


Figure 4. A DenseNet architecture with three (3) dense blocks [39]

3.1.4 Implementation details

The proposed DenseNets-121 model for COVID-19 detection is trained on Intel (R) Core (TM) i5-7200U TPU @2.75GHz, RAM (8 GB), and Python 3.8 version using Google Colab. The running time was 25 minutes for the training of 300 images.

We trained our network for 60 epochs using Adam optimizer with a constant learning rate of $1e-5$. The binary cross-entropy loss function was used to calculate the loss between predictions and real labels.

4. RESULTS AND DISCUSSIONS

4.1 Experiments results

Now that we have explained our methodology, we'll go on to the following section to talk about the model's performance in comparison to several cutting-edge models for diagnosing COVID-19 disease (Table 3).

We compute the accuracy, precision, recall, and F1-score to assess the performance of the suggested model. We provide a summary definition of the metrics and discuss how they relate

to our classification of novel COVID-19 disease in the paragraphs that follow. The following parameters are used to determine the metrics: TP, TN, FP, and FN stand for true positive, true negative, false positive and false negative, respectively.

Precision: it checks what proportion of positive identifications achieved by a model were actually correct and is given by (Eq. (3)).

$$\text{Precision} = \text{TP} / (\text{TP} + \text{FP}) \quad (3)$$

Recall: it checks the number of actual positive cases in our datasets which the proposed CNN model was able to correctly identify. This is given by (Eq. (4)).

$$\text{Recall} = \text{TP} / (\text{TP} + \text{FN}) \quad (4)$$

F1-Score: It expresses the balance between the precision and the recall described above and helps us decide whether the performance of our model is based on precision and recall. It is given by (Eq. (5)).

$$\text{F1-Score} = (2 * \text{Precision} * \text{Recall}) / (\text{Precision} + \text{Recall}) \quad (5)$$

Accuracy: Accuracy is a very popular metric that should only be used to compare distinct classes. The percentage of objects that have been accurately classified is clearly stated. It is the proportion of subjects with accurate labels to the entire group of topics. Accuracy is the most logical one (Eq. (6)).

$$\text{Accuracy} = (\text{TP} + \text{TN}) / (\text{TP} + \text{TN} + \text{FP} + \text{FN}) \quad (6)$$

Specificity is the correctly items labeled by the program to all who are positive in reality. (Eq. (7)).

$$\text{Specificity} = \text{TN} / (\text{TN} + \text{FP}) \quad (7)$$

To test the proposed approach, we evaluate our model using three different metrics for each of the classes: precision, recall and F1-score (Table 2).

Table 2. Precision, Recall, F1-score and Accuracy metrics for the proposed method

	Precision	Recall	F1-score
0	0.95	1.00	0.98
1	1.00	1.00	1.00
2	1.00	0.94	0.97
Accuracy		0.98	
Macro average		0.98	
Weighted average		0.98	

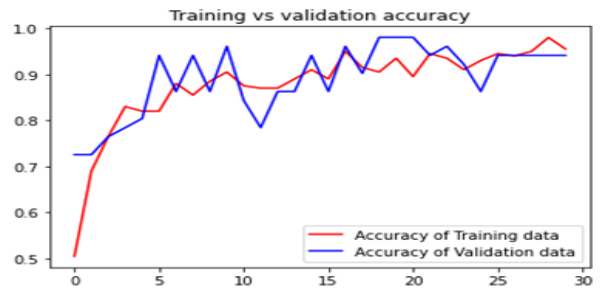


Figure 5. Accuracy of training and validation data vs. epochs

Table 3. Performances of other convolutional neural networks to detect COVID-19 comparing our approach

Approaches	Accuracy	Precision	F1-score	Recall	Specificity
ResNet50	93.53	96.01	94.56	96.6	90.31
InceptionV3	90.67	90.08	92.64	96.3	--
InceptionResNetV2	90.28	89.81	93.04	97.1	--
RBFNN	70.45	72.50	69.05	--	--
3SBBO	86.12	86.14	86.16	--	--
CovidResNet	82.46	78.67	79.35	--	--
CovidDenseNet	82.87	79.25	80.16	82.2	--
Our approach	98.0	98.33	98.33	98.0	--

The accuracy on the training set is 98% and on validation set is 98% within only 30 epochs as in Figure 5, which shows the strength of the model.

Now, if we test our model on an unseen data (Figure 6), it will correctly classify it. Since the model was not shown the images on the validation set before, the prediction is quite accurate.



Figure 6. Testing our model on unseen data gives the correct classification

4.2 Comparison of our method with other COVID-19 diagnosis state-of-the-art

Compared to other approaches, our model was more accurate to classify the COVID-19 chest X-ray images. Especially where we had a leak of dataset related to this newly pandemic. Our approach could outperform the following state-of-the-art: RBFNN [40], ResNet50, InceptionV3, InceptionResNetV2 [41], 3SBBO [22], CovidResNet [42] and CovidDenseNet [43].

Accuracy=98.00%

Precision=98.33%

F1-score=98.33%

Recall=98.00%

Specificity=96.64%

Min (TP/ (TP+FN), TN/ (TN+FP))=96.64%

5. CONCLUSIONS

The goal of this investigation is to achieve an early detection of COVID-19 from X-ray pictures using a PC-aided automated approach. In order to reduce the incidence of the virus, particularly in low-income countries, the scourge status conspiracy calls for the right X-ray examination for COVID-19 by deep learning algorithms. The view of COVID-19's X-

ray images further supports the value of a CAD framework. The CNN classifier declared the results to be satisfactory with a high level of 98 percent precision. Finally, this type of architecture would be absolutely necessary for the identification of COVID-19 and for enhancing radiologists' time and effort. The proposed methodology provided an unrevealed best alternative identification technique employing a DenseNet-121 CNN, theoretically contributing to the present growing COVID-19 literature. All succeeding layers can access the feature-maps discovered by any of the DenseNet-121 levels. This encourages models to be more compact and facilitates feature reuse across the network. Radiologists and professors can practically use this technique in clinical settings for precise COVID-19 detection. In order to capture a real-picture of infection rate, which has a high association to the number of daily-infected cases, boosting dependability represented through the proposed computational approach for testing could be valuable. The used methodology provided a potent machine learning-based strategy to reduce manual judgment errors made by professionals and provide a quicker way of offering time and resource saving. Applying various types of architecture, such as DenseNet-161, DenseNet-169, and DenseNet-201, can support DenseNet-121 for future research development. To identify COVID-19 patients more precisely, alternative deep learning techniques or modified deep learning techniques could be used and tested for future development and assessment.

AVAILABILITY OF DATA AND MATERIALS

The used data are available under [<https://drive.google.com/file/d/1odxJF4kyHEtBqhkqvz3iXpV3iQK34m6z0/view>] website and it is totally free and open access.

AUTHORS' CONTRIBUTIONS

KY designed the study, wrote the paper, managed the project, and was responsible for the final submission and revisions of the manuscript. MH configured the experimental environment, arranged experimental data and organized the datasets. KA did the statistical analysis and revised the paper. All the authors read and approved the submission of this paper.

ACKNOWLEDGMENT

We would like to thank Google for providing free and powerful GPU on Colab servers and free space on Google Drive. As well as the Python community and open access,

REFERENCES

[1] World Health Organization (WHO). Coronavirus statistics. <https://www.who.int/emergencies/diseases/novel-coronavirus-2019/situation-reports>, accessed on June 8, 2021.

[2] Huang, C., Wang, Y., Li, X., et al. (2020). Clinical features of patients infected with 2019 novel Coronavirus in Wuhan, China. *The Lancet*, 395(10223): 497-506. [https://doi.org/10.1016/S0140-6736\(20\)30183-5](https://doi.org/10.1016/S0140-6736(20)30183-5)

[3] Guan, W.J., Ni, Z.Y., Hu, Y., et al. (2020). Clinical characteristics of 2019 novel Coronavirus infection in China. *MedRxiv*. <https://doi.org/10.1056/NEJMoa2002032>

[4] Lei, J., Li, J., Li, X., Qi, X. (2020). CT imaging of the 2019 novel Coronavirus (2019-nCoV) pneumonia. *Radiology*, 295(1): 18-18. <https://doi.org/10.1148/radiol.2020200236>

[5] Song, F., Shi, N., Shan, F., Zhang, Z., Shen, J., Lu, H., Ling, Y., Jiang, Y., Shi, Y. (2020). Emerging 2019 novel Coronavirus (2019-nCoV) pneumonia. *Radiology*, 295(1): 210-217. <https://doi.org/10.1148/radiol.2020200274>

[6] Chung, M., Bernheim, A., Mei, X., Zhang, N., Huang, M., Zeng, X., Cui, J., Xu, W., Yang, Y., Fayad, Z.A., Jacobi, A., Li, K., Li, S., Shan, H. (2020). CT imaging features of 2019 novel Coronavirus (2019-nCoV). *Radiology*, 295(1): 202-207. <https://doi.org/10.1148/radiol.2020200230>

[7] Ardila, D., Kiraly, A.P., Bharadwaj, S., Choi, B., Reicher, J.J., Peng, L., Tse, D., Etemadi, M., Ye, W., Corrado, G., Naidich, D.P., Shetty, S. (2019). End-to-end lung cancer screening with three-dimensional deep learning on low-dose chest computed tomography. *Nature Medicine*, 25(6): 954-961. <https://doi.org/10.1038/s41591-019-0447-x>

[8] Suzuki, K. (2017). Overview of deep learning in medical imaging. *Radiological Physics and Technology*, 10(3): 257-273. <https://doi.org/10.1007/s12194-017-0406-5>

[9] Coudray, N., Ocampo, P.S., Sakellaropoulos, T., Narula, N., Snuderl, M., Fenyö, D., Moreira, A.L., Razavian, N., Tsirigos, A. (2018). Classification and mutation prediction from non-small cell lung cancer histopathology images using deep learning. *Nature Medicine*, 24(10): 1559-1567. <https://doi.org/10.1038/s41591-018-0177-5>

[10] Xu, X., Jiang, X., Ma, C., et al. (2020). A deep learning system to screen novel Coronavirus disease 2019 pneumonia. *Engineering*, 6(10): 1122-1129. <https://doi.org/10.1016/j.eng.2020.04.010>

[11] Esteva, A., Kuprel, B., Novoa, R.A., Ko, J., Swetter, S.M., Blau, H.M., Thrun, S. (2017). Dermatologist-level classification of skin cancer with deep neural networks. *nature*, 542(7639): 115-118. <https://doi.org/10.1038/nature21056>

[12] Wu, W., Xu, X., Jiang, X., Ma, C., et al. (2020). A deep learning system to screen novel Coronavirus disease 2019 pneumonia. *Engineering*, 6(10): 1122-1129. <https://doi.org/10.1016/j.eng.2020.04.010>

[13] Wang, X., Zheng, C., Deng, X., Fu, Q., Zhou, Q., Feng, J., Ma, H., Liu, W. (2020). Deep learning-based detection for COVID-19 from chest CT using weak label. *MedRxiv*, 2020-03. <https://doi.org/10.1109/TMI.2020.2995965>

[14] Chowdhury, M.E., Rahman, T., Khandakar, A., Mazhar, R., Kadir, M.A., Mahbub, Z.B., Islam, K.R., Khan, M.S., Iqbal, A., Al Emadi, N., Reaz, M.B.I., Islam, M.T. (2020). Can AI help in screening viral and COVID-19 pneumonia? *IEEE Access*, 8: 132665-132676. <https://doi.org/10.1109/ACCESS.2020.3010287>

[15] Gozes, O., Frid-Adar, M., Greenspan, H., Browning, P.D., Zhang, H., Ji, W., Bernheim, A., Siegel, E. (2020). Rapid ai development cycle for the Coronavirus (covid-19) pandemic: Initial results for automated detection & patient monitoring using deep learning CT image analysis. *arXiv preprint arXiv:2003.05037*. <https://doi.org/10.48550/arXiv.2003.05037>

[16] Dadário, A.M.V., Paiva, J.P.Q., Chate, R.C., Machado, B.S., Szarf, G. (2020). Regarding "artificial intelligence distinguishes COVID-19 from community acquired pneumonia on chest CT". *Radiology*. <https://doi.org/10.1148%2Fradial.2020201178>

[17] Yang, Y., Song, Y., Zheng, S., Li, L., Zhang, X., Zhang, X., Huang, Z., Chen, J., Wang, R., Zhao, H., Chong, Y., Shen, J., Zha, Y. (2021). Deep learning enables accurate diagnosis of novel Coronavirus (COVID-19) with CT images. *IEEE/ACM Transactions on Computational Biology and Bioinformatics*, 18(6): 2775-2780. <https://doi.org/10.1109/TCBB.2021.3065361>

[18] Xu, B., Wang, S., Kang, B., Ma, J., Zeng, X., Xiao, M., Guo, J., Cai, M., Yang, J., Li, Y., Meng, X. (2021). A deep learning algorithm using CT images to screen for Corona Virus Disease (COVID-19). *European Radiology*, 31: 6096-6104. <https://doi.org/10.1007/s00330-021-07715-1>

[19] Shi, Y., Shan, F., Gao, Y., Wang, J., Shi, W., Shi, N., Han, M., Xue, Z., Shen, D. (2020). Lung infection quantification of COVID-19 in CT images with deep learning. *arXiv preprint arXiv:2003.04655*. <https://doi.org/10.1002/mp.14609>

[20] Yu, H.G., Chen, J., Wu, L., Zhang, J., et al. (2020). Deep learning-based model for detecting 2019 novel Coronavirus pneumonia on high-resolution computed tomography. *Scientific Reports*, 10(1): 19196. <https://doi.org/10.1038/s41598-020-76282-0>

[21] Shen, D., Shi, F., Xia, L., Shan, F., Song, B., Wu, D., Wei, Y., Yuan, H., Jiang, H., He, Y. (2021). Large-scale screening to distinguish between COVID-19 and community-acquired pneumonia using infection size-aware classification. *Physics in Medicine & Biology*, 66(6): 065031. <https://doi.org/10.1088/1361-6560/abe838>

[22] Wang, W., Huang, X., Li, J., Zhang, P., Wang, X. (2021). Detecting COVID-19 patients in X-ray images based on MAI-nets. *International Journal of Computational Intelligence Systems*, 14(1) 1607-1616. <https://doi.org/10.2991/ijcis.d.210518.001>

[23] Wang, W., Liu, H., Li, J., Nie, H., Wang, X. (2021). Using CFW-Net deep learning models for X-ray images to detect COVID-19 patients. *International Journal of Computational Intelligence Systems*, 14(1): 199-207. <https://doi.org/10.2991/ijcis.d.201123.001>

[24] Wang, S.H., Wu, X., Zhang, Y.D., Tang, C., Zhang, X. (2020). Diagnosis of COVID-19 by wavelet Renyi

- entropy and three-segment biogeography-based optimization. *International Journal of Computational Intelligence Systems*, 13(1): 1332-1344. <https://doi.org/10.2991/ijcis.d.200828.001>
- [25] Sudowe, P., Leibe, B. (2016). Patchit: Self-supervised network weight initialization for fine-grained recognition. In *BMVC*, 1: 24-25. <https://dx.doi.org/10.5244/C.30.75>
- [26] Zhao, J., Zhang, Y., He, X., Xie, P. (2020). Covid-CT-dataset: A CT scan dataset about COVID-19. *arXiv preprint arXiv:2003.13865*, 2020.
- [27] Deng, J., Dong, W., Socher, R., Li, L.J., Li, K., Li, F. (2009). ImageNet: A large-scale hierarchical image database. In *2009 IEEE Conference on Computer Vision and Pattern Recognition*, Miami, FL, USA, pp. 248-255. <https://doi.org/10.1109/CVPR.2009.5206848>
- [28] Devlin, J., Chang, M.W., Lee, K., Toutanova, K. (2018). Bert: Pre-training of deep bidirectional transformers for language understanding. *arXiv preprint arXiv:1810.04805*.
- [29] Ren, S., He, K., Girshick, R., Sun, J. (2015). Faster R-CNN: Towards real-time object detection with region proposal networks. *Advances in Neural Information Processing Systems*, 28. <https://doi.org/10.48550/arXiv.1506.01497>
- [30] Huynh, B.Q., Li, H., Giger, M.L. (2016). Digital mammographic tumor classification using transfer learning from deep convolutional neural networks. *Journal of Medical Imaging*, 3(3): 034501-034501. <https://doi.org/10.1117/1.JMI.3.3.034501>
- [31] Raghu, M., Zhang, C., Kleinberg, J., Bengio, S. (2019). Transfusion: Understanding transfer learning for medical imaging. *Advances in Neural Information Processing Systems*, 32. <https://doi.org/10.48550/arXiv.1902.07208>
- [32] Chouhan, V., Singh, S.K., Khamparia, A., Gupta, D., Tiwari, P., Moreira, C., Damaševičius, R., de Albuquerque, V.H.C. (2020). A novel transfer learning based approach for pneumonia detection in chest X-ray images. *Applied Sciences*, 10(2): 559. <https://doi.org/10.3390/app10020559>
- [33] Elmahdy, M.S., Abdeldayem, S.S., Yassine, I.A. (2017). Low quality dermal image classification using transfer learning. In *2017 IEEE EMBS International Conference on Biomedical & Health Informatics (BHI)*, Orlando, FL, pp. 373-376. <https://doi.org/10.1109/BHI.2017.7897283>
- [34] Esteva, A., Kuprel, B., Novoa, R.A., Ko, J., Swetter, S.M., Blau, H.M., Thrun, S. (2017). Dermatologist-level classification of skin cancer with deep neural networks. *Nature*, 542(7639): 115-118. <https://doi.org/10.1038/nature21056>
- [35] Sudowe, P., Leibe, B. (2016). Patchit: Self-supervised network weight initialization for fine-grained recognition. In *BMVC*, 1: 24-25. <https://dx.doi.org/10.5244/C.30.75>
- [36] Ramani, R., Vanitha, N.S., Valarmathy, S. (2013). The pre-processing techniques for breast cancer detection in mammography images. *International Journal of Image, Graphics and Signal Processing*, 5(5): 47-54. <https://doi.org/10.5815/ijgisp.2013.05.06>
- [37] Belhaouari, S.B., Raissouli, H. (2021). Madl: a multilevel architecture of deep learning. *International Journal of Computational Intelligence Systems*, 14(1): 693-700. <https://doi.org/10.2991/ijcis.d.201216.003>
- [38] Huang, G., Liu, Z., van der Maaten, L., Weinberger, K.Q. (2017). Densely connected convolutional networks. In *Proceedings of the IEEE Conference on Computer Vision and Pattern Recognition*, Honolulu, pp. 4700-4708. <https://doi.org/10.1109/CVPR.2017.243>
- [39] Krizhevsky, A., Sutskever, I., Hinton, G.E. (2017). ImageNet classification with deep convolutional neural networks. *Communications of the ACM*, 60(6): 84-90. <https://doi.org/10.1145/3065386>
- [40] He, K., Zhang, X., Ren, S., Sun, J. (2016). Deep residual learning for image recognition. In *Proceedings of the IEEE Conference on Computer Vision and Pattern Recognition*, pp. 770-778. <https://doi.org/10.48550/arXiv.1512.03385>
- [41] Punn, N.S., Agarwal, S. (2021). Automated diagnosis of COVID-19 with limited posteroanterior chest X-ray images using fine-tuned deep neural networks. *Applied Intelligence*, 51(5): 2689-2702. <https://doi.org/10.1007/s10489-020-01900-3>
- [42] Das, N.N., Kumar, N., Kaur, M., Kumar, V., Singh, D. (2022). Automated deep transfer learning-based approach for detection of COVID-19 infection in chest X-rays. *IRBM*, 43(2): 114-119. <https://doi.org/10.1016/j.irbm.2020.07.001>
- [43] Alshazly, H., Linse, C., Abdalla, M., Barth, E., Martinetz, T. (2021). COVID-Nets: Deep CNN architectures for detecting COVID-19 using chest CT scans. *PeerJ Computer Science*, 7: e655. <https://doi.org/10.7717/peerj-cs.655>

NOMENCLATURE

RT-PCR	Reverse Transcription Polymerase Chain Reaction
AI	Artificial intelligence
CNN	Convolutional neural network thermal
CT	Chest computed tomography
DNN	Deep neural network
TP	True positive
TN	True negative
FP	False positive
FN	False negative